Plant Science 352 (2025) 112368

Contents lists available at ScienceDirect

Plant Science

journal homepage: www.elsevier.com/locate/plantsci

AtTRM11 as a tRNA 2-methylguanosine methyltransferase modulates flowering and bacterial resistance via translational regulation

Zhengyi Lv [a], Lun Guan [a], Ruixuan Yao [a], Hanchen Chen [e], Hailang Wang [b], Xukai Li [d], Xiaodong Xu [c], Liangcai Peng [b], Youmei Wang [d,*], Peng Chen [a,*]

[a] College of Plant Science & Technology, Huazhong Agricultural University, Wuhan, Hubei Province 430070, China
[b] School of Life and Health Sciences, Hubei University of Technology, Wuhan, Hubei Province 430068, China
[c] School of Life Science, Henan University, Kaifeng, Henan Province 475004, China
[d] Houji Laboratory in Shanxi Province, College of Agriculture, Shanxi Agricultural University, Taiyuan, Shanxi Province 030031, China
[e] Yazhouwan National Labratory, Sanya, Hainan Province 572025, China

ARTICLE INFO

Keywords:
Arabidopsis
TRNA
2-methylguanosine
TRM11
Translation control

ABSTRACT

2-methylguanosine is an eukaryote-specific modified nucleoside in transfer RNAs, and m^2G10 is catalyzed by Trm11-Trm112 protein complex in eukaryotic tRNAs. Here, we show that loss-of-function mutation of the *Arabidopsis* Trm11 homolog *AtTRM11* resulted in m^2G deficiency associated with disturbed ribosome assembly and overall transcriptome changes, including genes involved in flowering regulation and plant-pathogen interaction. The *attrm11* mutant showed phenotypes of enlarged rosette leaves and early flowering, as well as enhanced resistance to *Pseudomonas* bacterial infection. *AtTRM11* could partially rescue the m^2G nucleoside level in yeast *trm11* mutant, and AtTRM11 protein mostly resided in cytosol and physically interacted with AtTRM112b *in planta*. *AtTRM11* was mostly expressed in shoot apex, root tip, and distal end of rosette leaves. KEGG enrichment analysis of differentially expressed genes between *trm11* mutant and wild type indicated changes in pathways including phenopropanoid biosynthesis, plant-pathogen interaction, plant hormone signal transduction and MAPK signaling, suggesting that the pleiotropic phenotypes of the *attrm11* mutant can be ascribed to translational and transcriptional changes.

1. Introduction

Eukaryotic transfer RNAs contain modified nucleosides at different locations on the secondary cloverleaf structure (El Yacoubi et al., 2012; Dunin-Horkawicz et al., 2006; Bjork et al., 1987). The presence of modified nucleoside can alter the local base-pairing strength and therefore influence the tertiary structure of the whole tRNA molecule and codon recognition during the decoding process (Gruber et al., 2010; Agris et al., 2007). 2-methylguanosine (m^2G) is a methylated modification present on certain snRNA, rRNA and tRNA species in organisms of Archaea and Eukarya kingdoms (Bourgeois et al., 2016; Purushothaman et al., 2005; Guy and Phizicky, 2014; Armengaud et al., 2004). In tRNAs, the enzymes catalyzing the m^2G or m^2_2G modification work independently, and in some cases, m^2G can be further methylated to N2, N2-dimethylguanosine (m^2_2G) (El Yacoubi et al., 2012; Purushothaman et al., 2005; Liu and Straby, 2000).

The first m^2G methyltransferases identified in eukaryotes are Trm11p and Trm112p from *Saccharomyces cerevisiae* (Purushothaman et al., 2005). Genetic evidence has suggested that both enzymes are required for m^2G modification at position 10 in tRNA-Ile-UAU and tRNA-Phe-GAA. In the latter case, the interaction of m^2G10 and m^2_2G26 modification respectively mediated by Trm11-Trm112 and Trm1 contributes to the tertiary structure stability of tRNA-Phe (Purushothaman et al., 2005). Yeast Trm11p was found to be mostly located in the cytoplasm and nearly not in the nucleus (Purushothaman et al., 2005). Mutation in the associated protein Trm112 led to more growth reduction due to its association with other enzymes such as Trm9p, Lys9p and Mtc6p (Purushothaman et al., 2005; Heurgue-Hamard et al., 2006; Mazauric et al., 2010). Recently, Yang et al. showed that a human THUMP-domain containing protein 3 (THUMPD3) is activated by

* Corresponding authors.
E-mail addresses: 601921044@qq.com (Z. Lv), 826944837@qq.com (L. Guan), 136593116@qq.com (R. Yao), chenhanchen@yzwlab.cn (H. Chen), 836916637@qq.com (H. Wang), xukai_li@sxau.edu.cn (X. Li), xiaodong.xu@henu.edu.cn (X. Xu), lpeng@mail.hzau.edu.cn (L. Peng), wym@sxau.edu.cn (Y. Wang), chenpeng@mail.hzau.edu.cn (P. Chen).

https://doi.org/10.1016/j.plantsci.2024.112368
Received 8 September 2024; Received in revised form 11 December 2024; Accepted 20 December 2024
Available online 22 December 2024

interacting with HsTRMT112 for m^2G modification on a broad range of tRNA substrates (Yang et al., 2021). The Trm9-Trm112 complex is responsible for $mcm^5(s2)U$ wobble uridine modification, whereas the Mtq2-Trm112 complex mediates the methylation of eRF1, which is involved in translation termination (Mazauric et al., 2010; Studte et al., 2008; Gavin et al., 2002). As an allosteric regulator, human TRMT112 contributes to the biogenesis of 40S ribosome via m^7G1636 and m^6A1832 methylation on 18S rRNA mediated by the complex formed from WBSCR22 (Bud23 in *S. cerevisiae*) and METTL5 (no homolog found in *S. cerevisiae*) (Bourgeois et al., 2016; Figaro et al., 2012; Letoquart et al., 2014). Interaction with ALKBH8 (Trm9 in yeast) contributes to cm^5U-related wobble uridine modification of some tRNAs, and cm^5U itself is mediated by the elongator complex (Fu et al., 2010). Global interactome analysis revealed that Trm112 is connected with even more protein members, and most of these members are associated with ribosome biogenesis and translation (Bourgeois et al., 2016; Studte et al., 2008).

Notably, the archaeal Trm11 from *T. kodakarensis* and *P. abyssi* is capable of m^2G and even m_2^2G modification without a Trm112 partner (Armengaud et al., 2004; Hirata et al., 2016; Urbonavicius et al., 2006). Several studies have revealed the specific structural information of archaeal Trm11 proteins, and archaeal Trm14 from *Pyrococcus furiosus* had the most similar structure to Trm11, which catalyzes the formation of m^2G6 in certain archaeal tRNA species (Hirata et al., 2016; Fislage et al., 2012; Wang et al., 2020). In *M. jannaschii*, both m^2G6 and m^2G67 were identified, which consist of a base-pair on the acceptor stem (Yu et al., 2019). m^2G67 has also been identified in *HeteroLoligo bleekeri* (Matsuo et al., 1995). m^2G67 is present in the tRNA-Trp-CCA of *Thermococcus kodakarensis*, tRNA-Lys of *Loligo bleekeri*, and tRNA-Arg, tRNA-Asn, tRNA-Gly, tRNA-Ile and tRNA-Val of *Methanococcus jannaschii* (Yu et al., 2019; Matsuo et al., 1995). It currently remains unclear whether aTrm14 is capable of methylating both m^2G6 and m^2G67 on the same tRNA isoacceptor. A "molecular ruler" model has been proposed by structural modelling of aTrm11 proteins for m^2G/m_2^2G10 methylation and aTrm14 proteins for m^2G6 methylation (Hirata et al., 2016).

Eukaryotes need different enzymes for m^2G or m_2^2G. For example, Trm1 is responsible for m^2G/m_2^2G26 in *S. cerevisiae* (Liu and Straby, 2000), and Trm11-Trm112 catalyzes m^2G10 formation (Purushothaman et al., 2005). The intense interaction between Trm11 and Trm112 protein is mediated by hydrophobic interaction, and structural studies have suggested coordinated movement of the sub-domain of Trm11 driven by Trm112 upon substrate tRNA binding (Bourgeois et al., 2017). Accordingly, the MTase domain of Trm11 homologs contains the (D/N/S)PP(F/Y/W/H) motif required for modifying exocyclic amines from bases or glutamine side chains (Heurgue-Hamard et al., 2006; Bujnicki, 2000). The human Trm112 protein TRMT112 was identified as the hub of an MTase network, and can form protein complex with TRMT11, THUMPD3, and THUMPD2 respectively, to form m^2G10 and m^2G6 on tRNAs or m^2G72 on U6 snRNA (Wang et al., 2023). The *T. kodakarensis* ⊿*trm11* mutant showed poor growth performance at high temperature, suggesting the importance of m_2^2G10 in maintaining tRNA structure stability at high temperatures (van Tran et al., 2018). The *Arabidopsis TRM112* homolog *AtTRM112B(AtSMO2)* is highly expressed in root tip, shoot apex and young siliques, and the *smo2* mutant displayed smaller aerial organs and shorter roots due to reduced cell proliferation (Hu et al., 2010).

In our previous work, we have identified a T-DNA knock-out mutant of *AtTRM11* in *Arabidopsis thaliana* and found that its loss-of-function mutation led to m^2G deficiency (Chen et al., 2010). In addition, we found that *AtTRM11* expression was temporally induced by heat, drought or salt treatment (http://www.bar.utoronto.ca/efp/cgi-bin), and significantly up-regulated by cold stress (Wang et al., 2017), suggesting that it may be a stress indicator. In this study, we further investigated the interaction of AtTRM11 with AtTRM112 and their function in regulating plant development and disease response. Our results showed that dysfunction of *AtTRM11* influenced the overall ribosomal composition and translation, and also altered the transcription of genes related to flowering initiation and plant-pathogen interaction. The translational and transcriptional changes resulting from tRNA-m^2G deficiency eventually led to pleiotropic phenotypes.

2. Material and methods

2.1. Plant growth conditions

Arabidopsis Columbia-0 ecotype was used in this study. The seeds were either first sterilized by ethanol and germinated on 1/2 MS medium until the roots were 1 cm long and transferred to soil pots, or directly sown in pots containing soil and vermiculite (3: 1 v/v) in a greenhouse at 16 h photoperiod, 22 °C/18 °C (day/night temperature) with 150 $\mu mol/m^{-2}s^{-1}$ light intensity and 60 % humidity. The *At3g26410 (AtTRM11)* Salk line T-DNA *Salk_122158* was purchased from the European *Arabidopsis* Stock Centre (NASC, http://arabidopsis.info). T-DNA lines were genotyped using primers binding to the T-DNA left or right border combined with gene-specific internal primers (T-DNA primer design tool, http://signal.salk.edu/tdnaprimers.2.html).

Plant flowering time was monitored by the percentage of bolting plants after direct planting in soil. For each genotype, at least 50 individual plants were cultivated. The leaf length and leaf width were measured with the 6–7th rosette leaves of 4-week-old plants.

2.2. Promoter-GUS assay for tissue-specific expression of AtTRM11

A 3.0-kb genomic sequence upstream of the *AtTRM11* start codon was amplified and cloned into gateway vector pHGWFS7 (https://vectorvault.vib.be/collection/phgwfs7) (Karimi et al., 2002) with GUS as reporter for promoter activity. The recombinant vector pHGWSF7-AtTRM11pmt-GUS was transformed into GV3101 *Agrobacterium* and used for generation of transgenic plants with hygromycin as selective marker. Positive T1 seeds were selected and propagated in the greenhouse to obtain homozygous T2 transgenic lines. Tissues were collected subsequently from T3 homozygous transgenic plant for GUS assay.

Rosette leaves, roots, and shoot apex were examined from two-week-old or six-week-old *Arabidopsis* plants. Tissues were incubated in X-gluc reaction solution (1 mM X-gluc, 50 mM sodium phosphate, pH 7.0, 0.1 % Triton X-100, 1 mM potassium ferricyanide and 1 mM potassium ferrocyanide) in a dark incubator at 37 °C overnight, and decolored the next day with 70 % (v/v) ethanol before examination under a stereomicroscope (Leica S6D, Germany).

2.3. Pseudomonas AvrRpt2 infection and disease phenotyping

Pto DC3000 strain carrying the avrRpt2 effector was kindly provided by Dr. Kenichi Tsuda from Huazhong Agricultural University. The strain was cultured in KB medium at 28 °C at 200 rpm overnight and subcultured the next day in the same medium to $OD_{600} = 0.6$ (exponential growth phase). The bacterial cells were harvested by centrifugation, washed once and re-suspended to $OD_{600} = 0.2$ with suspension buffer (containing 10 mM magnesium chloride, pH 5.6). PtoDC3000 (avrRpt) strain was further diluted with suspension buffer to OD600 = 0.002, and ca. 100 μL bacterial culture was infiltrated with a needleless syringe to the back side of four fully grown rosette leaves. The same bacterial suspension was used for five individual plants as biological replicates. The infected leaves were harvested 72 h post infection. Leave discs were collected from each infected leaves, and the bacterial growth assay was performed according to Nobori et al. (2020).

2.4. tRNA isolation and nucleoside analysis by LC-MS

Small RNAs were extracted using microRNA Extraction Kit (Omega Bio-tek Inc.). RNA concentration was determined using NanoDrop ND-

1000 spectrophotometer (Thermo Scientific). About 20 μg tRNA was digested with P1 nuclease (Sigma) and Calf Intestine Alkaline Phosphatase as described previously (Wang et al., 2017). Samples were diluted with Milli-Q water (Millipore Synergy) to a concentration of 10 μg mL^{-1} and the injection volume was 10 μL.

A UPLC-MS/MS system was used for nucleoside separation and quantification. API 4000 Q-Trap mass spectrometer (Applied Biosystems) was used with an LC-230A UPLC system and a diode array UV detector (190 −400 nm). ESI-MS was conducted in the positive ion mode. The nebulizer gas, auxiliary gas, curtain gas, turbo gas temperature, entrance potential, and ion spray voltage were 60 psi, 65 psi, 15 psi, 550 °C, 10 and 5500 V, respectively. Inertsil ODS-3 column (2.1 mm × 150 mm, 5 μm particle size; Shimadzu) was used for nucleoside separation. The mobile phase gradient was as follows (Yan et al., 2013): 0–10 min, 0–50 % solvent B; 10–13 min, 50–100 % solvent B; 13–23 min, 100 % solvent B; 23–23.1 min, 100–5 % solvent B; 23.1–30 min, 5–0 % solvent B. The flow rate was 0.6 mL/min at ambient temperature. Multiple reaction monitoring (MRM) mode was used for parent-to-product ion transitions. The identity of 2-methylguanosine was confirmed with its relative retention time and the Q1/Q3 ions of *m/z* 298.27/166.27 (Wang et al., 2017; Yan et al., 2013; Chan et al., 2010).

2.5. Protein subcellular localization

AtTRM11-eGFP vector was constructed using pD1301S with D35S and a C-terminal eGFP fragment inserted using *Sal*I and *Pst*I sites. The coding sequence (without stop codon) of AtTRM11 was PCR amplified and cloned in frame with downstream eGFP to create a 3'GFP tagged AtTRM11-eGFP protein. The recombinant construct was sequenced and transferred into Agrobacteria strain GV3101. The Agro strain carrying AtTRM11-eGFP was grown in liquid medium and infiltrated into lower epidermal cells of four-week-old *Nicotiana benthamiana* leaves. For better resolution, we also prepared protoplast from infiltrated tobacco leaves using a wall-degrading enzyme mix (20 mM MES, pH5.7, containing 1.5 % (w/v) cellulose R10, 0.4 % (w/v) macerozyme R10, 0.4 M mannitol and 20 mM KCl) (Yoo et al., 2007). Protein subcellular localization was visualized using a confocal laser scanning microscope (Leica SP5 CLSM) with × 63 objective lens. The excitation and emission wavelengths for DAPI were 385 and 420 nm, respectively; and 470–490 nm and 500–540 nm for GFP, respectively.

2.6. BiFC and split-LUC assay

For BiFC assays, the full-length CDS of *AtTRM11* and *AtTRM112b* without stop codon was amplified with the following primer pairs: TRM11-F, 5'-ggggacaagtttgtacaaaaaagcaggcttcATGTGGTTTCTGTGTGTCTT-3', TRM11-R, 5'-ggggaccactttgtacaagaaagctgggtcCACATACTTCCCTCTATACTTA-3', TRM112B-F, 5'-ggggacaagtttgtacaaaaaagcaggcttcATGAGGTTGATAACGCACAA-3', and TRM112B-R, 5'-ggggaccactttgtacaagaaagctgggtcAACCTCGTCTTCATGGAGAA-3'. These two PCR fragments (AtTRM11-no stop codon, AtTRM112b-no stop codon) were subsequently cloned into pEarleyGateYN (nYFP-tagged) and pEarleyGateYC (cYFP-tagged) respectively by homologous recombination (Chen et al., 2023). The resulting vectors were transformed into *Agrobacterium tumefaciens* strain GV3101 for tobacco leave transient transformation. YFP fluorescence was detected after 3 days of infiltration by a confocal microscope (Leica SP8).

For split-LUC assays, the full-length CDS of AtTRM11 or AtTRM112b was amplified and cloned into JW771 (Gene-nLUC orientation) or JW772 (cLUC-Gene orientation) vectors, respectively, using homologous recombination method (Chen et al., 2023). The resulting vectors were transformed into GV3101 strain before infiltration into *N. benthamiana* leaves at an OD600 of 0.6. Two days after infiltration, the leaf luciferase was monitored by a low-light cooled CCD imaging apparatus (Lumazone CA).

2.7. RNAseq and qRT-PCR

Four-week-old rosette leaves from *attrm11* mutant or Col.0 wild-type plants were taken in triple replicates for RNAseq analysis. Sequence reads were quality checked, mapped to the *Arabidopsis* reference genome and gene expression values for each expressed gene were compared pairwise to identify DEGs (differentially expressed genes). GO and KEGG enrichment analyses were performed for DEGs. Genes for flowering control or plant-pathogen interaction were validated by qRT-PCR. RNA extraction and reverse transcription were performed with the RNAprep pure Plant Kit (Tiangen Biotech, Beijing, China) and M-MLV RTase (TaKaRa, Dalian, China), respectively. qRT-PCR was conducted using a BioRad IQ5™ real-time PCR system (Life Science, Wuhan, China), with *At5g60390* (*AtEF1a*) and *At1g13440* (*AtGAPC2*) as reference genes (Jin et al., 2019). The $2^{\Delta\Delta Ct}$ method was used for calculating the relative expression (Livak and Schmittgen, 2001).

2.8. Polysome profiling

The basic procedures for polysome profiling were conducted according to Ingolia et al. (2012). Healthy 4-week-old or six-true-leaf *Arabidopsis* seedlings were used as the starting material. Then, 350–500 mg leaves were pulverized in a mortar with liquid nitrogen, transferred to a 10-mL glass tissue grinder, followed by the addition of 1 mL plant lysis buffer (200 mM Tris-HCl, pH8.4, 50 mM KCl, 25 mM $MgCl_2$, 1 % deoxycholate, 2 % polyoxyethylene 10 tridecyl ether, 50 μg/mL cycloheximide, 300 μg/mL heparin, 1 % Triton X-100, 1 % Tween 20, in RNase free water). The plant tissue was homogenized and transferred to an Eppendorf tube and incubated on ice for 15 min. A 15–45 % sucrose gradient was prepared and loaded with BIOCOMP Gradient Master ip-107 on centrifuge tubes compatible with the Beckman Coulter SW40 Ti rotor. All centrifugation steps were performed at 4°C. After first centrifugation at 20,000 g for 15 min, the supernatant was transferred to a new tube and measured for absorbance at 260 nm. Before second centrifugation, all samples were adjusted to the same A_{260} values with 15 % sucrose, and 1 mL of sample was loaded again on the sucrose gradient and centrifuged with BECKMAN Optima L-80 XP Ultracentrifuge at 36,000 rpm for 5 h. The ribosomal fractions separated by sucrose gradient were monitored by A_{254} from the bottom up and collected in fractions according to their density. A_{254} curves as a function of fraction separation were printed on a Pharmacia LKB REC-2 recorder (Ingolia et al., 2012). The peaks corresponding to 40 s, 60 s, 80 s and polysomes were annotated according to Holmes et al., by using the same base line for WT and *attrm11* mutant. Total RNA was extracted from fractions containing the 40 s/60 s, 80 s, or polysomes, and qRT-PCR was performed to check the transcript levels of target genes, using 18 s ribosomal RNA as the internal reference.

3. Results

3.1. AtTRM11 is a m^2G methyltransferase in Arabidopsis

Our lab has developed the first tRNA nucleoside analysis platform in *Arabidopsis* and rice (Chen et al., 2010; Wang et al., 2017; Wang et al., 2017; Jin et al., 2019), and also investigated the biological significance of various nucleoside modifications on plant tRNAs, especially for the adaptation of plants to environmental stimuli and also their own developmental requirement.

Based on protein sequence homology with Trm11p as a 2-methylguanosine methyltransferase in *S. cerevisiae*, we identified At3g26410 (AtTRM11) as a TRM11 homolog in *A. thaliana* (Chen et al., 2010). We then compared AtTRM11 protein with homologs from eukaryotes and archaea. As a result, plant Trm11 proteins were clearly clustered separately from those mammals, fungi, and archaea (Fig. 1a). AtTRM11 belongs to the Rossmann-fold superfamily with a RFM domain and an N-terminal THUMP domain (Fig. 1b, Suppl Fig. 1). LC-MS analysis of

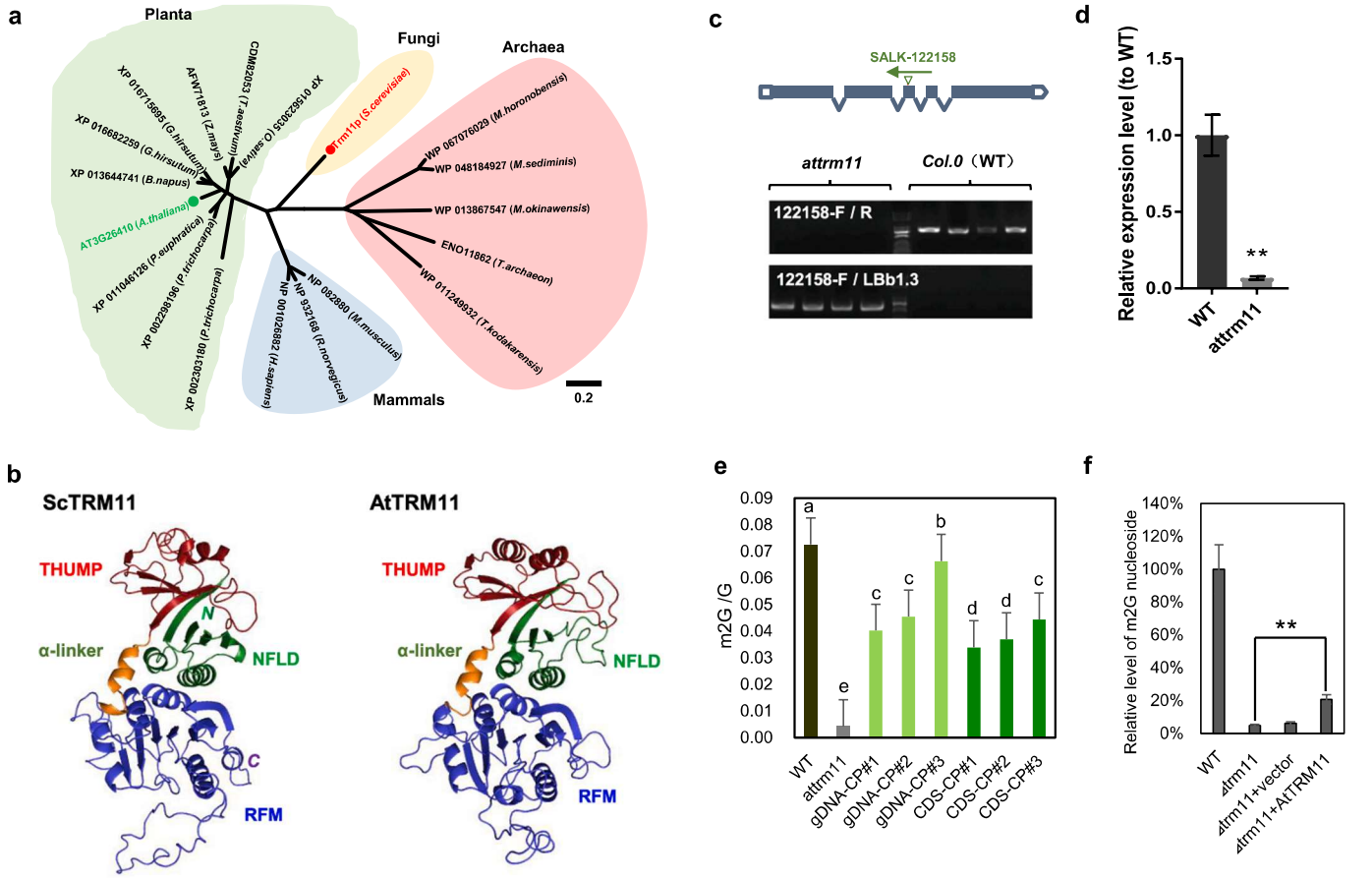

Fig. 1. AtTRM11 is a methyltransferase for tRNA m^2G methylation. (a) Phylogenic tree of Trm11 homologs in representative eukaryotic organisms. Color code indicates organism within plant (green), Archaea (rose), Fungi (yellow) and mammals (blue). AtTrm11 or At3g26410 is shown in green font. (b) Tertiary structure of the AtTrm11 protein showing the NFLD domain, the THUMP domain, and the Rossman Fold Methyltransferase (RFM) domain. (c) Genotyping of *attrm11* mutant with T-DNA insertion flanking sequence primers (122158-F/R) or in combination with T-DNA border primers (122158-F/LBb1.3). The expected size for PCR product is 775 bp for Col.0 with 122158-F/R, and 564 bp for *attrm11* with 122158-F/LBb1.3. (d) *AtTRM11* relative expression in WT and *attrm11* mutant. (e) m^2G nucleoside level quantified by LC-MS in mutant and complemented plants (CP) with gDNA or CDS, respectively. Different letters represent statistical difference by multi-variant analysis. (f) Yeast mutant complementation by AtTRM11. *Δtrm11*, yeast mutant (Y06274 from Euroscarf); WT, Y26274, congenic wild type for Y06274. Vector, pYPGE15 vector. m^2G nucleoside quantified by LC-MS.

nucleoside digested from total tRNAs also confirmed ca. 90 % reduction of m^2G level in the homozygous T-DNA mutant compared with the wild type (Fig. 1c-d, Suppl Fig. 2). When the mutant was complemented with plasmid carrying either the gDNA or cDNA of *AtTRM11*, the m^2G nucleoside level was partially recovered (Fig. 1e). In addition, *AtTRM11* could partially rescue *S. cerevisiae trm11* mutant with m^2G modification defect, suggesting that the function of MTase is conserved between *Arabidopsis* and yeast Trm11 proteins (Fig. 1f).

3.2. *AtTRM11 is a cytosolic protein interacting with AtTRM112b*

In a previous study, Hu et al. reported AtSmo2/AtTRM112b (At1g22270) as a Trm112 homolog in *Arabidopsis* (Hu et al., 2010). Indeed, there are two Trm112p homologs in *Arabidopsis*, among which AtSmo2 (AtTRM112b) shares 78 % protein sequence similarity to At1g78190 (AtTRM112a) (van Tran et al., 2018). However, based on the eFP data (http://bar.utoronto.ca/efp/cgi-bin/), *At1g78190* (*AtTRM112a*) had extremely low transcript levels in all tissues and therefore may be a pseudo-gene. Hence, we focused on *At1g22270* (*AtTRM112b*) instead for possible interaction with AtTRM11.

According to the SUBA (https://suba.live/) prediction, AtTRM11 protein is located in the mitochondria, while AtTRM112b is located in cytosol (Suppl Fig. 3a). However, through tobacco leaf transient transformation, we found that GFP-tagged AtTRM11 (GFP on C-terminal) was primarily located in the cytoplasm (Fig. 2a, Suppl Fig. 3b). The protein location of AtTRM11 in cytosol suggests its possible interaction with AtTRM112 to form a protein complex for m^2G formation by the Trm11p-Trm112p complex in other eukaryotic systems (Purushothaman et al., 2005; Wang et al., 2020; Bourgeois et al., 2017).

We then employed the BiFC system to test the interaction between AtTRM11 and AtTRM112b. Positive signals were found in the cytoplasm of transfected tobacco epidermis cells for the combination of AtTRM11-nYFP+AtTRM112-cYFP, while no signal was observed for either AtTRM11-nYFP or AtTRM112-cYFP alone (Fig. 2b). Meanwhile, the split luciferase assay also showed positive luciferase signals when tobacco leaves were co-infiltrated with AtTRM11-nLUC and cLUC-AtTRM112b (Fig. 2c), confirming the presence of the AtTRM11-TRM112b complex *in planta*. Based on the promoter-GUS results, we found that *AtTRM11* was highly expressed in shoot apex, root tip, and leaf proximal regions (Fig. 2d–e). The proper m^2G modification in these tissues may have important physiological functions.

3.3. *attrm11 mutant shows early flowering with transcriptional changes in key flowering regulators*

The Salk_122158 T-DNA mutant of *AtTRM11* gene exhibited an early flowering phenotype, and its bolting date was approximately 12 days earlier than that of *Col.0* (Fig. 3a-b). The *attrm11* mutant had larger and

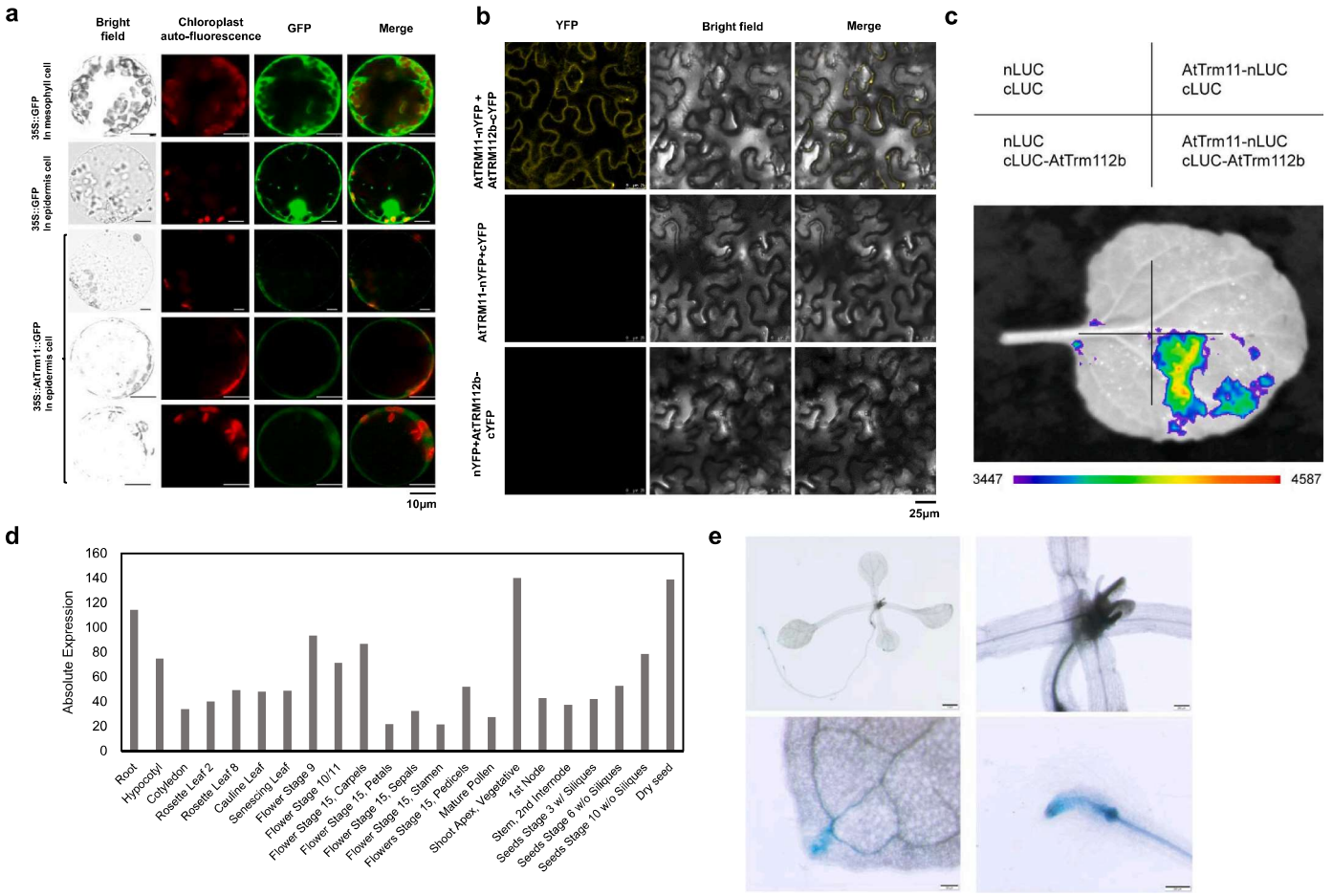

Fig. 2. AtTRM11 is cytosolic protein that interacts with AtTRM112b. (a) Protoplast tobacco leaf cells for GFP-tagged AtTRM11 protein subcellular localization. Panels from left to right, Bright field, Chloroplast auto-fluorescence, GFP channel, Merge picture of the second and third panels. Scale bar, 10 μm. (b) BiFC assay for interaction between AtTRM11 and AtTRM112b. Scale bar, 25 μm. (c) Split-LUC assay for AtTRM11-AtTRM112b interaction using tobacco leave infiltration. (d) AtTRM11 gene expression data from eFP database (https://bar.utoronto.ca/efp/). (e) Promoter-GUS assay for tissues positive for AtTRM11 gene expression. Scale bar, 200 μm.

wider rosette leaves than the wild type, suggesting its accelerated vegetative growth (Fig. 3c–e). Indeed, *AtTRM11*-OE plants also exhibited early flowering, though the flowering date was not as early as that of the *attrm11* mutant (Fig. 3b). On possible explanation is that the excess or absence of AtTRM11 may lead to improper assembly of the AtTRM11-AtTRM112b complex, which may have different functions for m^2G methylation and flowering control.

To identify the target genes responsible for the early flowering phenotype, we performed RNAseq of the four-week-old seedlings of *attrm11* mutant and *Col.0* wild type (Fig. 3f–g, Suppl Table 1). In a total of ca. 5300 DEGs, 2065 were up-regulated and 3326 were down-regulated (Fig. 3f). Fig. 3g shows that some genes in photoperiod and autonomous pathways were differentially expressed in the mutant compared with in the wild type. For example, *FT* as a flowering-indicator (Putterill and Varkonyi-Gasic, 2016) and *AGL24* as a flowering promoting gene (Michaels et al., 2003) had higher expression in the *attrm11* mutant, while *FLC*, a key flowering repressor, and its complex partner *SVP* had lower expression in the mutant (Fig. 3g). qRT-PCR validated that the transcript level of *FLC* and *SVP* was inhibited in the *attrm11* mutant, while that of *FT* and *AGL24* was up-regulated (Fig. 3h–k). Interestingly, the transcripts of some circadian-clock associated genes (such as *PRR9*, *CCA1* and *GI*) were also significantly altered in the *attrm11* mutant in RNAseq data. However, the circadian rhythmicity of *CCA1*, *LHY*, and *PRR9* transcripts was not detected by qRT-PCR under free-running conditions, suggesting that AtTRM11 does not directly regulate the circadian clock (Suppl Fig. 4).

3.4. *attrm11 is more resistant to Pseudomonas infection*

KEGG enrichment analysis of the RNAseq data identified DEGs in the pathways of phenylpropanoid biosynthesis, plant-pathogen interaction, and plant hormone signal transduction (Fig. 4a, Suppl Table 2). Indeed, the functional annotation of many top DEGs was related to plant-immune response, including genes and transcription factors related to lignin biosynthesis and phytohormone genes. We then investigated the immune response phenotype through *Pseudomonas* DC3000-AvrRpt2 strain infection on rosette leaves. The results showed that the *attrm11* mutant had less bacterial multiplication than the wild type after leaf infection (Fig. 4b-c). In terms of gene expression levels, we found that a set of genes from the calmodulin-like proteins (*AtCMLs* and *AtCNGCs*), *AtEDS1*, *AtBAK1*, *AtRboHC* and *AtRboHF*, several MAPKKK, MKKs and WRKY transcription factors (such as *AtWRKY29* and *AtWRKY33*), lignin biosynthesis genes (*CADs*, *4CL* and *PALs*), and a couple of phytohormone-related genes were significantly up-regulated in the *attrm11* mutant (Fig. 4d). We hypothesized that the improved resistance to *Pseudomonas* infection might be indirectly attributed to the translational/transcriptional changes of these target genes/proteins, which led to cell wall lignification and induction of JA and SA as well as Ca^{++} mediated defense response. However, since the m^2G defect is not likely to be specific for unique protein and pathways, it is difficult to pinpoint which target gene/protein(s) are mostly affected by m^2G modification deficiency. We then quantified the relative expression of *RboHF*, *WRKY29*, *PYL5* and *JAZ10* and found that the qRT-PCR results were

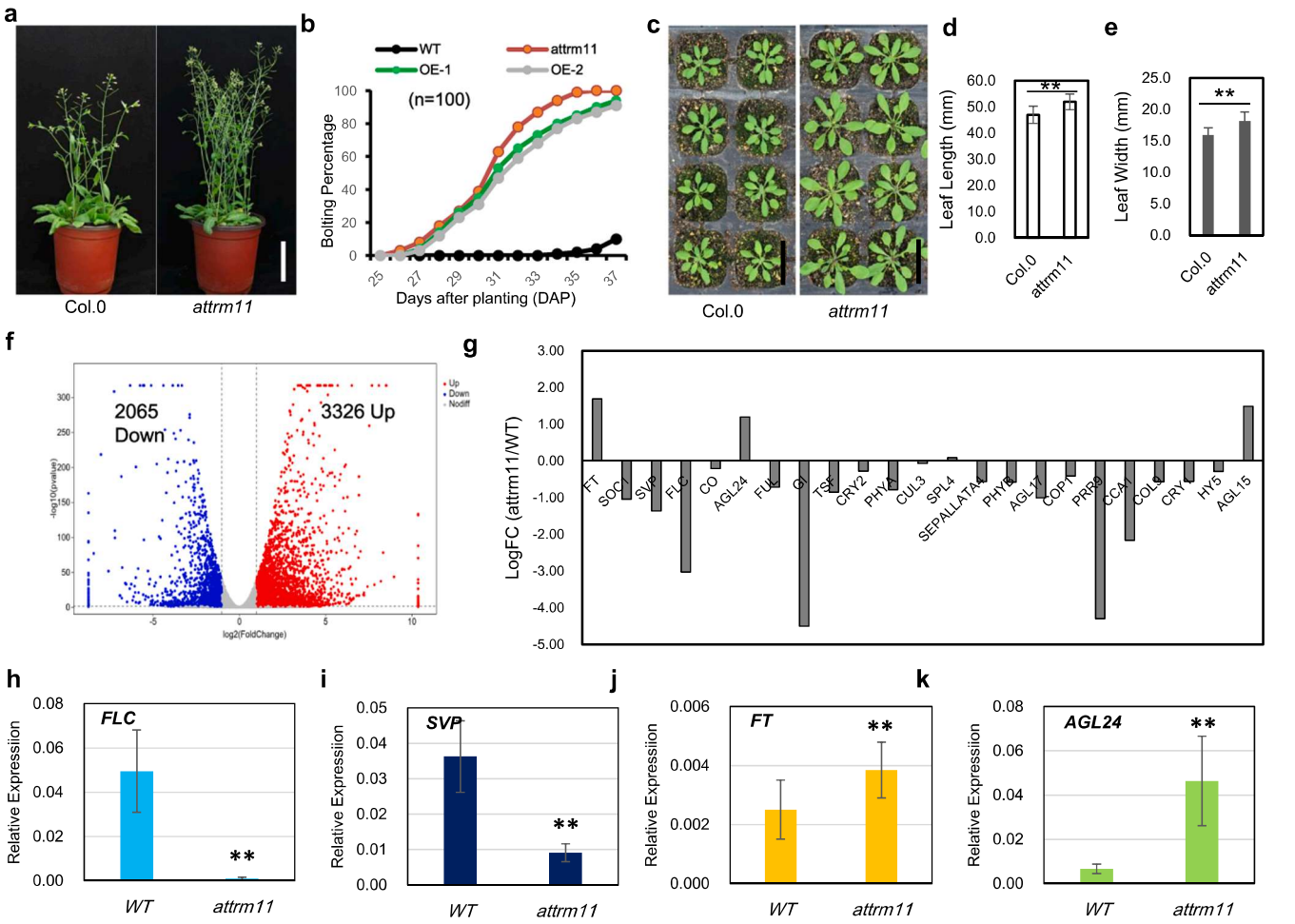

Fig. 3. *attrm11* mutant showed early flowering and accelerated rosette growth. (a) Plants at bolting stage. Left, wild type (Col.0); Right, *attrm11* mutant. Scale bar, 5 cm. (b) Bolting time comparison between *attrm11* mutant, AtTRM11-OE plants and wild type. n = 100, number of plant individuals tested for scoring bolting percentage from each genotype. (c) Rosette leaves of WT and *attrm11* mutant at 4 weeks old. Scale bar, 5 cm. (d-e) Length and Width of the average rosette leaves in WT (Col.0) and *attrm11* mutants. (f) Volcano plot of DEGs (differential expressed genes) from RNAseq. Blue dots indicates down-regulated genes, red dots represents up-regulated genes. (g) Log2FC (Fold of Change) for flowering regulator genes from RNAseq data. (h-k) qRT-PCR verification of *FT*, *FLC*, *SVP* and *AGL24* gene expression levels in WT (Col.0) and *attrm11* mutant.

consistent with the RNAseq data (Fig. 4e–h).

3.5. *attrm11 mutant has more dissociated ribosomes indicative of translation disturbance*

The most important biological role of tRNA modification is to ensure efficient and accurate translation to support cell growth and individual development. The substrate tRNAs of 2-methyltransferase include both cytosolic and mitochondrial tRNAs. Indeed, dysfunction of a subset of tRNAs in cellular compartments may greatly endanger the translation apparatus. We then used polysome profiling to compare the ribosomal subunit compositions from cell extracts and found that the ribosomes from the *attrm11* mutant had higher portions of 40 s and 60 s subunits (Fig. 5b), indicating a less functional translating ribosomes. We also performed qRT-PCR on RNAs extracted from polysome fractions to investigate transcript levels on translating ribosomes in wild type and *attrm11* mutant (Fig. 5c). The results showed that in translating polysomes, the transcript level of *FT* was higher in the *attrm11* mutant than in the wide type, which is consistent with the RNAseq data. The transcript levels of *FLC* and *SVP* were also higher in the *attrm11* mutant, while *AGL24* transcript was lower, which is not consistent with the RNAseq data and early-flowering phenotype of the *attrm11* mutant (Fig. 3h-i, k). On the other hand, polysome qRT-PCR data for the immune pathway genes (*RboHF*, *WRKY29*, *PYL5* and *JAZ10*) were generally consistent with the RNAseq data. The higher transcript level of these genes such as *RboHF* in *attrm11* mutant is consistent with the elevated resistance of the plant to *Pseudomonas* infection (Fig. 5c, Fig. 4e–h).

4. Discussion

A previous study has proposed a "molecular ruler" model when comparing the m^2G10 methylation by Trm11-Trm112 complex and m^2G6 by Trm14 in archaea (Hirata et al., 2016). According to the proposed model, the distance between the 3'CCA end and the to-be-methylated site in the tRNA substrates was measured by the "molecular ruler" composed of the THUMP domain and MTase domain from the Trm11 protein. Trm112 may be involved in stabilization of the anticodon loop and therefore improve the stability of the conformation between the associated tRNA substrates and the Trm11-Trm112 protein complex (Bourgeois et al., 2016).

Although the 3D structure of AtTRM11 protein or AtTRM11-AtTRM112 protein complex has not been unveiled, the conservation of amino acids such as the D(P/Y)PY motif and those predicted or identified as AdoMet-interacting residues supports the function of the complex as tRNA 2-methylguanosine methyltransferase (Hirata et al., 2016;

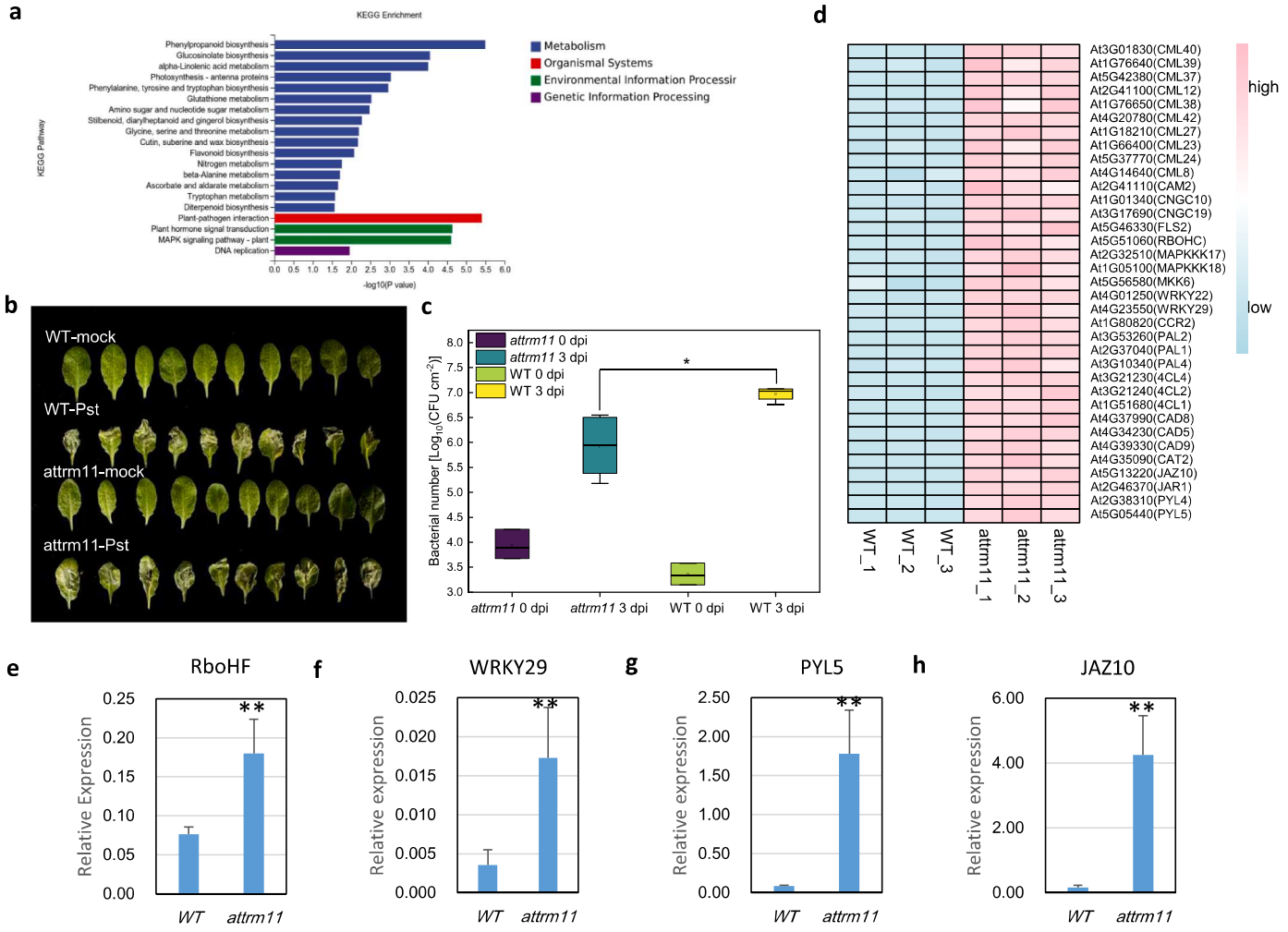

Fig. 4. Differential expression of defence related genes contributes to better resistance of *attrm11* mutant towards *Pseudomonas* infection. (a) KEGG enrichment of DEGs between *attrm11* and wild type. (b) *Pseudomonas* (AvrRpt2) infection on rosette leaves of *attrm11* and wild type. (c) Colony forming unit (CFU) comparison between *attrm11* and wild type before (T0) or 3 days (T3) after *Pseudomonas* (AvrRpt2) leave infection. (d) RNAseq data for up-regulated defence related genes in *attrm11* mutant. (e-h) qRT-PCR validation of relative expression of *RboHF*, *WRKY29*, *PYL5* and *JAZ10* genes in WT and *attrm11* mutant.

Wang et al., 2020) (Suppl Fig. 1). Surprisingly, the subcellular localization of AtTRM11 in the cytosol supports its partnership with AtTRM112b, and the AtTRM11-TRM112b complex could therefore methylate most tRNA substrates once they are transcribed and transported out of the nucleus. However, there are numerous mitochondrial tRNAs that contain m^2G10 modification, including tRNA-Leu-UAG from *Homo sapiens*, tRNA-Lys-CUU from *Loligo bleekeri*, tRNA-Leu-NAG (N, unknown modification) from *Phaseolus vulgaris*. It remains unclear whether these tRNAs are modified by the cytosolic Trm11 protein or other mitochondrial enzymes (Modomics database, https://genesilico.pl/modomics/). However, since the m^2G nucleoside abundance in our Arabidopsis *attrm11* mutant is less than 10 % of that in the wild type, AtTRM11 acts as the major m^2G methyltransferase for all tRNA substrates in cytosol and subcellular compartments.

One suppressing result of *attrm11* mutant was the flowering phenotype of *AtTRM11* over-expression in Col.0 background was also early flowering, similar to *attrm11* mutant (Fig. 3b). On the side, the lack of m^2G modification could be rescued by complementing plasmid carrying the complete coding sequence of *AtTRM11* gene (Fig. 1e). Therefore it seems the flowering phenotype could not be resulting from lack of m^2G nucleoside, not solely on translation level neither by transcriptional regulation. By the current study we could not identify all target genes/proteins affected by *attrm11* mutation. However we could generate another loss-of-function mutant of *AtTRM11* by CRISPR-Cas9 technology to see if *AtTRM11*-loss-of-function leads to changes on flowering initiation.

The qRT-PCR results from polysome fractions were not in good agreement with the RNAseq data, especially for the *FLC* and *SVP* genes, which are key flowering repressors. One reason might be their very low expression levels in certain samples from polysome fractions, leading to great fluctuations and eventually difficulty in data interpretation (Fig. 5c). In addition, these results also highlight the importance of polysome profiling to study translation regulation, since the loading of target transcripts on translating ribosomes might be more critical than the transcript level. The m^2G deficiency resulting from *attrm11* mutation led to accelerated rosette growth and bolting, as well as better bacterial resistance to *Pseudomonas* infection. The RNA-seq results showed that approximately 10–15 % of all genes (2065 + 3326 = 5391, the total number of genes in Arabidopsis genome is ca. 25,000) were either up- or down-regulated (Fig. 3f), which might be caused by secondary effects from translational changes. Indeed, the transcription factors FT and FLC for flowering regulation or WRKY22 and WRKY29 for plant-pathogen interaction were differentially expressed, which might be mediated by decoding changes on codons involving m^2G-containing tRNAs. According to the Modomics database, the following tRNA isoacceptors might contain m^2G at position 10, including tRNA-Ala-IGC, tRNA-Arg-ICG,

a

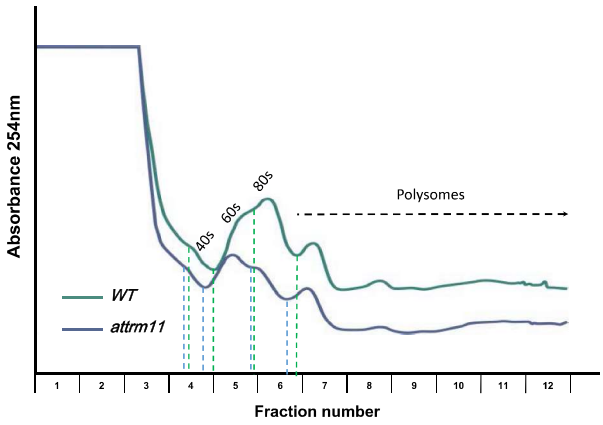

b

	WT	attrm11
40s+60s	15.70 (24.9%)	11.95 (42,0%)
80s	10.79 (17.1%)	4.08 (14.3%)
Polysome	36.45 (57.9%)	12.44 (43.7%)
Mono : Poly	1.00 : 3.37	1.00 : 3.05

c

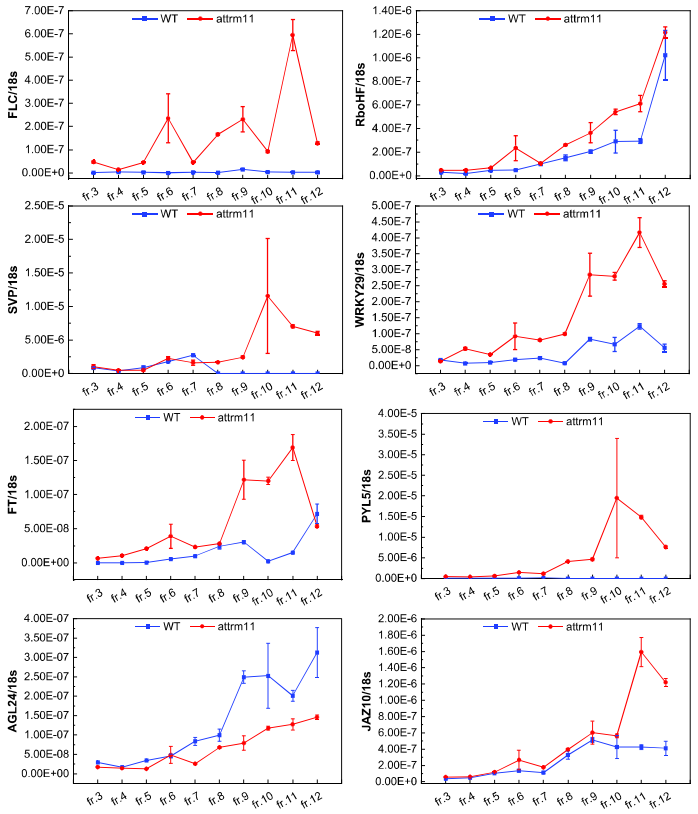

Fig. 5. *attrm11* mutant has less portion of 80 s ribosomes for successful translating apparatus. (a) Polysome profiling for ribosome samples collected from 4 weeks-old seedlings of attrm11 mutant and wild type. The approximate elution fraction for the 40 s, 60 s and 80 s ribosomes were indicated. (b) Quantified peak areas for the 40 s, 60 s, 80 s and polysomes in wildtype and attrm11 mutant. Blue dashed line indicated annotation of peaks corresponding to 40 s, 60 s,80 s or polysomes from attrm11 sample, green dashed line indicated annotation for WT sample. The same base line was used for wildtype and attrm11 samples. (c) qRT-PCR for selected genes in flowering control or plant immune response in RNAs extracted from polysome fractions from attrm11 mutant and wild type.

tRNA-Asn-GUU, tRNA-Asp-QUC (Q as queosine), tRNA-Gln-CUA, tRNA-Gly-GCC, tRNA-Ile-IAU (I as inosine), tRNA-iMet, tRNA-Leu-IAG/-UAG/-CAG/-CAA, tRNA-Lys-CUU, tRNA-Phe-GAA/-#AA (# as 2'-O-methylguanosine), tRNA-Tyr-QUA/-GPA (P as pseudouridine), and tRNA-Val-UAC (Suppl Table 3). We calculated the codon frequency for UUU and UUC codons (Phe), UUA, UUG and CUN codons (Leu) within the CDS regions of RboHC, WRKY22, WRKY29, 4CL1, PAL1, FT, FLC and SVP. As a result, no direct correlation was found between codon frequency and gene expression (Suppl Fig. 5). Without proteomics data and direct measurement of the decoding efficiency on specific codons, it is so far difficult to explain the connection between m^2G10 deficiency on a certain protein target and protein abundance.

In this study, we investigated the interaction of AtTRM11 with AtTRM112 to form a protein complex for m^2G methylation and their potential role in plant development and disease response. Our results highlight the critical role of m^2G modification in tRNA, influencing not only ribosome assembly and translation but also development and stress response pathways in *Arabidopsis*. The interplay between m^2G modification and gene expression provides insights into the complex regulatory mechanisms underpinning plant biology, paving avenues for further research on the roles of RNA modification in various physiological contexts. Future studies may be focused on dissecting the specific pathways affected by m^2G deficiency and exploring the potential of manipulating these modifications to enhance plant resilience and adaptability.

CRediT authorship contribution statement

Ruixuan Yao: Investigation, Formal analysis, Data curation. **Hanchen Chen:** Methodology, Investigation, Data curation. **Zhengyi Lv:** Conceptualization. **Lun Guan:** Formal analysis, Data curation. **Xiaodong Xu:** Writing – review & editing, Investigation, Data curation. **Liangcai Peng:** Writing – review & editing, Investigation. **Hailang Wang:** Methodology, Investigation, Data curation. **Xukai Li:** Software, Data curation. **Youmei Wang:** Writing – review & editing, Project administration, Funding acquisition, Data curation, Conceptualization. **Peng Chen:** Writing – review & editing, Supervision, Project administration, Funding acquisition, Data curation, Conceptualization.

Declaration of Competing Interest

We hereby state that this work described has not been published previously, and it is not under consideration for publication elsewhere. This submission is approved by all authors and the work carried out here will not be published elsewhere in the same form without the written consent of the copyright-holder.

Acknowledgements

This work was supported by the National Natural Science Foundation of China (32000381 to WYM, 31100268 and 32372171 to PC). We are grateful for Dr. Kenichi Tsuda for providing the Pto DC3000 (avrRpt2) strain. We thank Dr. Shunping Yan (Huazhong Agricultural University) for providing vectors and technical support for the BiFC and Split-LUC assay.

Appendix A. Supporting information

Supplementary data associated with this article can be found in the online version at doi:10.1016/j.plantsci.2024.112368.

Data availability

Data will be made available on request.

References

P.F. Agris, F.A. Vendeix, W.D. Graham, tRNA's wobble decoding of the genome: 40 years of modification, J. Mol. Biol. 366 (1) (2007) 1–13, https://doi.org/10.1016/j.jmb.2006.11.046.

J. Armengaud, J. Urbonavičius, B. Fernandez, G. Chaussinand, J.M. Bujnicki, H. Grosjean, N2-Methylation of Guanosine at Position 10 in tRNA Is Catalyzed by a THUMP Domain-containing, S-Adenosylmethionine-dependent Methyltransferase, Conserved in Archaea and Eukaryota, J. Biol. Chem. 279 (35) (2004) 37142–37152, https://doi.org/10.1074/jbc.M403845200.

G.R. Bjork, J.U. Ericson, C.E. Gustafsson, T.G. Hagervall, Y.H. Jonsson, P.M. Wikstrom, Transfer RNA modification, Annu. Rev. Biochem. 56 (1987) 263–287, https://doi.org/10.1146/annurev.bi.56.070187.001403.

G. Bourgeois, J. Letoquart, N. van Tran, M. Graille, Trm112, a protein activator of methyltransferases modifying actors of the eukaryotic translational apparatus, Biomolecules 7 (1) (2017), https://doi.org/10.3390/biom7010007.

G. Bourgeois, J. Marcoux, J.-M. Saliou, S. Cianférani, M. Graille, Activation mode of the eukaryotic m2G10tRNA methyltransferase Trm11 by its partner protein Trm112, Nucleic Acids Res. (2016) gkw1271, https://doi.org/10.1093/nar/gkw1271.

J.M. Bujnicki, Phylogenomic analysis of 16S rRNA:(guanine-N2) methyltransferases suggests new family members and reveals highly conserved motifs and a domain structure similar to other nucleic acid amino-methyltransferases, FASEB J.: Off. Publ. Fed. Am. Soc. Exp. Biol. 14 (14) (2000) 2365–2368, https://doi.org/10.1096/fj.00-0076com.

C.T. Chan, M. Dyavaiah, M.S. DeMott, K. Taghizadeh, P.C. Dedon, T.J. Begley, A quantitative systems approach reveals dynamic control of tRNA modifications during cellular stress, PLoS Genet. 6 (12) (2010) e1001247, https://doi.org/10.1371/journal.pgen.1001247.

P. Chen, G. Jager, B. Zheng, Transfer RNA modifications and genes for modifying enzymes in Arabidopsis thaliana, BMC Plant Biol. 10 (2010) 201, https://doi.org/10.1186/1471-2229-10-201.

G. Chen, D. Xu, Q. Liu, Z. Yue, B. Dai, S. Pan, Y. Chen, X. Feng, H. Hu, Regulation of FLC nuclear import by coordinated action of the NUP62-subcomplex and importin β SAD2, J. Integr. Plant Biol. 65 (9) (2023) 2086–2106, https://doi.org/10.1111/jipb.13540.

S. Dunin-Horkawicz, A. Czerwoniec, M.J. Gajda, M. Feder, H. Grosjean, J.M. Bujnicki, MODOMICS: a database of RNA modification pathways, Nucleic Acids Res 34 (2006), https://doi.org/10.1093/nar/gkj084. D145-149.

B. El Yacoubi, M. Bailly, V. de Crecy-Lagard, Biosynthesis and function of posttranscriptional modifications of transfer RNAs, Annu. Rev. Genet 46 (2012) 69–95, https://doi.org/10.1146/annurev-genet-110711-155641.

S. Figaro, L. Wacheul, S. Schillewaert, M. Graille, E. Huvelle, R. Mongeard, C. Zorbas, D. L. Lafontaine, V. Heurgue-Hamard, Trm112 is required for Bud23-mediated methylation of the 18S rRNA at position G1575, Mol. Cell. Biol. 32 (12) (2012) 2254–2267, https://doi.org/10.1128/MCB.06623-11.

M. Fislage, M. Roovers, I. Tuszynska, J.M. Bujnicki, L. Droogmans, W. Versees, Crystal structures of the tRNA:m2G6 methyltransferase Trm14/TrmN from two domains of life, Nucleic Acids Res. 40 (11) (2012) 5149–5161, https://doi.org/10.1093/nar/gks163.

Y. Fu, Q. Dai, W. Zhang, J. Ren, T. Pan, C. He, The AlkB domain of mammalian ABH8 catalyzes hydroxylation of 5-methoxycarbonylmethyluridine at the wobble position of tRNA, Angew. Chem. Int Ed. Engl. 49 (47) (2010) 8885–8888, https://doi.org/10.1002/anie.201001242.

A.C. Gavin, M. Bosche, R. Krause, P. Grandi, M. Marzioch, A. Bauer, J. Schultz, J.M. Rick, A.M. Michon, C.M. Cruciat, et al., Functional organization of the yeast proteome by systematic analysis of protein complexes, Nature 415 (6868) (2002) 141–147, https://doi.org/10.1038/415141a.

A. Gruber, S. Strobl, B. Veit, W. Oberhuber, Impact of drought on the temporal dynamics of wood formation in Pinus sylvestris, Tree Physiol. 30 (4) (2010) 490–501, https://doi.org/10.1093/treephys/tpq003.

M.P. Guy, E.M. Phizicky, Two-subunit enzymes involved in eukaryotic post-transcriptional tRNA modification, RNA Biol. 11 (12) (2014) 1608–1618, https://doi.org/10.1080/15476286.2015.1008360.

V. Heurgue-Hamard, M. Graille, N. Scrima, N. Ulryck, S. Champ, H. van Tilbeurgh, R. H. Buckingham, The zinc finger protein Ynr046w is plurifunctional and a component of the eRF1 methyltr ansfer ase in yeast, J. Biol. Chem. 281 (2006) 36140–36148.

A. Hirata, S. Nishiyama, T. Tamura, A. Yamauchi, H. Hori, Structural and functional analyses of the archaeal tRNA m2G/m22G10 methyltransferase aTrm11 provide mechanistic insights into site specificity of a tRNA methyltransferase that contains common RNA-binding modules, Nucleic Acids Res. 44 (13) (2016) 6377–6390, https://doi.org/10.1093/nar/gkw561.

M.J. Holmes, J. Misra, R.C. Wek, Analysis of translational control in the integrated stress response by polysome profiling, in: D. Matějů, J.A. Chao (Eds.), The Integrated Stress Response. Methods in Molecular Biology, 2022, 157-17.

Z. Hu, Z. Qin, M. Wang, C. Xu, G. Feng, J. Liu, Z. Meng, Y. Hu, The Arabidopsis SMO2, a homologue of yeast TRM112, modulates progression of cell division during organ growth, Plant J.: Cell Mol. Biol. 61 (4) (2010) 600–610, https://doi.org/10.1111/j.1365-313X.2009.04085.x.

N.T. Ingolia, G.A. Brar, S. Rouskin, A.M. McGeachy, J.S. Weissman, The ribosome profiling strategy for monitoring translation in vivo by deep sequencing of ribosome-protected mRNA fragments, Nat. Protoc. 7 (8) (2012) 1534–1550, https://doi.org/10.1038/nprot.2012.086.

X. Jin, Z. Lv, J. Gao, R. Zhang, T. Zheng, P. Yin, D. Li, L. Peng, X. Cao, Y. Qin, et al., AtTrm5a catalyses 1-methylguanosine and 1-methylinosine formation on tRNAs and is important for vegetative and reproductive growth in Arabidopsis thaliana, Nucleic Acids Res. 47 (2) (2019) 883–898, https://doi.org/10.1093/nar/gky1205.

M. Karimi, D. Inze, A. Depicker, GATEWAY vectors for Agrobacterium-mediated plant transformation, Trends Plant Sci. 7 (5) (2002) 193–195, https://doi.org/10.1016/s1360-1385(02)02251-3.

J. Letoquart, E. Huvelle, L. Wacheul, G. Bourgeois, C. Zorbas, M. Graille, V. Heurgue-Hamard, D.L. Lafontaine, Structural and functional studies of Bud23-Trm112 reveal 18S rRNA N7-G1575 methylation occurs on late 40S precursor ribosomes, Proc. Natl. Acad. Sci. USA 111 (51) (2014) E5518–5526, https://doi.org/10.1073/pnas.1413089111.

J. Liu, K.B. Straby, The human tRNA(m(2)(2)G(26))dimethyltransferase: functional expression and characterization of a cloned hTRM1 gene, Nucleic Acids Res 28 (18) (2000) 3445–3451, https://doi.org/10.1093/nar/28.18.3445.

K.J. Livak, T.D. Schmittgen, Analysis of relative gene expression data using real-time quantitative PCR and the 2(-Delta Delta C(T)) Method, Methods 5 (4) (2001) 402–408, https://doi.org/10.1006/meth.2001.1262.

M. Matsuo, T. Yokogawa, K. Nishikawa, K. Watanabe, N. Okada, Highly specific and efficient cleavage of squid tRNA(Lys) catalyzed by magnesium ions, J. Biol. Chem. 270 (17) (1995) 10097–10104, https://doi.org/10.1074/jbc.270.17.10097.

M.H. Mazauric, L. Dirick, S.K. Purushothaman, G.R. Björk, B. Lapeyre, Trm112p is a 15-kDa zinc finger protein essential for the activity of two tRNA and one protein methyltransferases in yeast, J. Biol. Chem. 285 (24) (2010) 18505–18515.

S.D. Michaels, G. Ditta, C. Gustafson-Brown, S. Pelaz, M. Yanofsky, R.M. Amasino, AGL24 acts as a promoter of flowering in Arabidopsis and is positively regulated by vernalization, Plant J. 33 (5) (2003), https://doi.org/10.1046/j.1365-313x.2003.01671.x, 867-74.

T. Nobori, Y. Wang, J. Wu, S.C. Stolze, Y. Tsuda, I. Finkemeier, H. Nakagami, K. Tsuda, Multidimensional gene regulatory landscape of a bacterial pathogen in plants, Nat. Plants 6 (7) (2020) 883–896, https://doi.org/10.1038/s41477-020-0690-7.

S.K. Purushothaman, J.M. Bujnicki, H. Grosjean, B. Lapeyre, Trm11p and Trm112p are both required for the formation of 2-methylguanosine at position 10 in yeast tRNA, Mol. Cell. Biol. 25 (11) (2005) 4359–4370.

J. Putterill, E. Varkonyi-Gasic, FT and florigen long-distance flowering control in plants, Curr. Opin. Plant Biol. 33 (2016) 77–82, https://doi.org/10.1016/j.pbi.2016.06.008.

P. Studte, S. Zink, D. Jablonowski, C. Bär, T. von der Haar, M.F. Tuite, R. Schaffrath, tRNA and protein methylase complexes mediate zymocin toxicity in yeast, Mol. Microbiol. 69 (5) (2008) 1266–1277.

N. van Tran, L. Muller, R.L. Ross, R. Lestini, J. Letoquart, N. Ulryck, P.A. Limbach, V. de Crecy-Lagard, S. Cianferani, M. Graille, Evolutionary insights into Trm112-methyltransferase holoenzymes involved in translation between archaea and eukaryotes, Nucleic Acids Res. 46 (16) (2018) 8483–8499, https://doi.org/10.1093/nar/gky638.

J. Urbonavicius, J. Armengaud, H. Grosjean, Identity elements required for enzymatic formation of N2,N2-dimethylguanosine from N2-monomethylated derivative and its possible role in avoiding alternative conformations in archaeal tRNA, J. Mol. Biol. 357 (2) (2006) 387–399, https://doi.org/10.1016/j.jmb.2005.12.087.

Y. Wang, D. Li, J. Gao, X. Li, R. Zhang, X. Jin, Z. Hu, B. Zheng, S. Persson, P. Chen, The 2′-O-methyladenosine nucleoside modification gene OsTRM13 positively regulates salt stress tolerance in rice, J. Exp. Bot. 68 (7) (2017) 1479–1491, https://doi.org/10.1093/jxb/erx061.

Y. Wang, C. Pang, X. Li, Z. Hu, Z. Lv, B. Zheng, P. Chen, Identification of tRNA nucleoside modification genes critical for stress response and development in rice and Arabidopsis, BMC Plant Biol. 17 (1) (2017) 261, https://doi.org/10.1186/s12870-017-1206-0.

C. Wang, N. van Tran, V. Jactel, V. Guerineau, M. Graille, Structural and functional insights into Archaeoglobus fulgidus m2G10 tRNA methyltransferase Trm11 and its Trm112 activator, Nucleic Acids Res. 48 (19) (2020) 11068–11082, https://doi.org/10.1093/nar/gkaa830.

C. Wang, N. Ulryck, L. Herzel, N. Pythoud, N. Kleiber, V. Guérineau, V. Jactel, C. Moritz, Markus T. Bohnsack, C. Carapito, et al., N2-methylguanosine modifications on human tRNAs and snRNA U6 are important for cell proliferation, protein translation and pre-mRNA splicing, Nucleic Acids Res. 51 (14) (2023) 7496–7519, https://doi.org/10.1093/nar/gkad487.

M. Yan, Y. Wang, Y. Hu, Y. Feng, C. Dai, J. Wu, D. Wu, F. Zhang, Q. Zhai, A high-throughput quantitative approach reveals more small RNA modifications in mouse liver and their correlation with diabetes, Anal. Chem. 85 (24) (2013) 12173–12181, https://doi.org/10.1021/ac4036026.

W.Q. Yang, Q.P. Xiong, J.Y. Ge, H. Li, W.Y. Zhu, Y. Nie, X. Lin, D. Lv, J. Li, H. Lin, et al., THUMPD3-TRMT112 is a m2G methyltransferase working on a broad range of tRNA

substrates, Nucleic Acids Res. 49 (20) (2021) 11900–11919, https://doi.org/10.1093/nar/gkab927.
S.D. Yoo, Y.H. Cho, J. Sheen, Arabidopsis mesophyll protoplasts: a versatile cell system for transient gene expression analysis, Nat. Protoc. 2 (7) (2007) 1565–1572, https://doi.org/10.1038/nprot.2007.199.
N. Yu, M. Jora, B. Solivio, P. Thakur, C.G. Acevedo-Rocha, L. Randau, V. de Crecy-Lagard, B. Addepalli, P.A. Limbach, tRNA modification profiles and codon-decoding strategies in Methanocaldococcus jannaschii, J. Bacteriol. 201 (9) (2019), https://doi.org/10.1128/JB.00690-18.